

1 **Supplementary Materials and Methods**

2 **Immunofluorescence**

3 Larvae were dissected in batches of 5-20 in PBS at room temperature and transferred to ice. Samples
4 were then fixed in PBS plus 4% paraformaldehyde (Electron Microscopy Services) for 25-minutes at
5 room temperature on an orbital shaker. Fixed samples were washed in PBS + 0.15% Triton X100 (PBT).
6 Antibodies were incubated either for 2hrs at room temperature or overnight at 4°C. After secondary
7 antibody incubation, samples were washed once with PBT, once with PBT + 0.2µg / ml DAPI, and once
8 with PBT. The following antibody concentrations were used: 1:750 mouse anti-EcR (DSHB DDA2.7,
9 concentrate), 1:4000 rabbit anti-GFP (Abcam ab290), 1:3500 mouse anti-Dl (DSHB C594.9b,
10 concentrate), 1:200 mouse anti-FLAG M2 (Sigma F1804), 1:1000 anti-Br (DSHB 25E9.D7,
11 concentrate), 1:500 anti-Dcp-1 (Cell Signaling Technology 9578). Secondary antibodies were: 1:1000
12 goat anti-rabbit, or goat anti-mouse, conjugated with either Alexa-488 or Alexa-594 (ThermoFisher
13 A11037, A11034). Samples were imaged on a Leica Sp5 or Leica Sp8 confocal microscope. Salivary
14 gland DNA content and dimensions were measured using the ROI manager in FIJI.

15 **Sample preparation for RNA-Seq**

16 A minimum of 60 wings or salivary glands were prepared as previously described (58) from either
17 *Oregon R (WT)* or *yw; vg-GAL4, tub>CD2>GAL4, UAS-GFP, UAS-FLP / UAS-EcR-RNAi¹⁰⁴ (EcR-*
18 *RNAi)*. For library construction, 50-100ng RNA was used as input to the Tecan Genomics Universal
19 RNA-Seq with NuQuant, Drosophila. Library preparation followed the manufacturer's instructions with
20 the following modifications: 1) after second-strand cDNA synthesis, samples were sonicated 5x20-
21 seconds (30-seconds rest between cycles) on high power in a BioRupter bath sonicator; 2) qPCR was
22 performed to determine the optimal cycle number using manufacturer's recommendations; 3) after library
23 amplification, an additional, 1.2:1 SPRI bead-cleanup was performed. Paired-end, 2x75 sequencing was
24 performed on an Illumina HiSeq X using Novogene Co.

25 **Sample preparation for CUT&RUN**

26 A minimum of 75 wings or 50 salivary glands from *w; EcR^{GFSTF}/Df(2R)BSC313* were dissected in wash
27 buffer (20mM HEPES-NaOH, 150mM NaCl, 2mM EDTA, 0.5mM Spermidine, 10mM PMSF). The rest
28 of the protocol was performed as described in¹. Fragments that diffused out of the nucleus (“supernatant”
29 sample), as well as size-selected DNA from the nuclei (“pellet” samples) were prepared and sequenced.
30 For library preparation, the Takara ThruPLEX DNA-seq kit with unique dual-indexes was used following
31 the manufacturer’s protocol until the amplification step. For amplification, after the addition of indexes,
32 16-21 cycles of 98C, 20s; 67C, 10s were run. A 1.2x SPRI bead cleanup was performed (Agencourt
33 Ampure XP). Libraries were sequenced on an Illumina HiSeq 4000 with 2x75 reads. The following
34 antibody concentrations were used: 1:300 mouse anti-FLAG M2; 1:200 rabbit anti-Mouse (Abcam
35 ab46450); 1:400 Batch#6 protein A-MNase (gift of Steven Henikoff).

36 **Sample preparation for FAIREseq**

37 Larvae from either *Oregon R (WT)* or *yw; vg-GAL4, tub>CD2>GAL4, UAS-GFP, UAS-FLP / UAS-EcR-*
38 *RNAi¹⁰⁴ (EcR-RNAi)* were dissected in 1xPBS in batches of 5-10 then fixed at RT for 10-minutes in 4%
39 paraformaldehyde, 50mM HEPES (pH 8.0), 100mM NaCl, 1mM EDTA (pH 8.0), 0.5mM EGTA (pH
40 8.0). Fixation was quenched by incubation for 5m in 1xPBS, 125mM Glycine, 0.01% Triton X-100 and
41 then transferred to 10mM HEPES (pH 8.0), 10mM EDTA (pH 8.0), 0.5mM EGTA (pH 8.0), 0.25% Triton
42 X-100, 1mM PMSF. Wings or salivary glands were dissected off cuticles and snap frozen in liquid
43 nitrogen. Samples were lysed in 2% Triton X-100, 1% SDS, 100mM NaCl, 10mM Tris (pH 8.0), 1mM
44 EDTA. Following lysis, a minimum of 40 wings or salivary glands were pooled together and
45 homogenized using 2.38mm tungsten beads with 6 cycles of 1min on and 2min off and then sonicated
46 using a Branson Sonifier with 5 cycles of 30-seconds (1-second on, 0.5-second off) while letting the
47 samples rest for at least 2-minutes on ice between cycles. An aliquot was removed as an input fraction.
48 The remaining samples were subjected to phenol-chloroform and chloroform extractions and then

49 precipitated with ethanol. Input and experimental samples were heated overnight at 65°C to reverse cross
50 links and then treated with RNase A for 1-hour at 37°C. DNA was purified with a Qiagen QIAquick PCR
51 Purification Kit eluting in nuclease free water. Samples were used as input into the Takara ThruPLEX
52 DNA-seq kit following manufacturer's instructions.

53 **RNA Sequencing Analysis**

54 Reads were trimmed using bbmap (v38.75) with parameters ktrim=r ref=adapters rcomp=t tpe=t tbo=t
55 hdist=1 mink=11. Reads were aligned with STAR (2.7.3a)². Indexes for STAR were generated with
56 parameter --sjdbOverhang 74 using genome files for the dm6 reference genome. The STAR aligner was
57 run with parameters --alignIntronMax 50000 --alignMatesGapMax 50000. Samtools (v1.9) was used to
58 filter reads to those with a q-score greater than 2. RSubread (v2.0.1) was used to count reads mapping to
59 genes using a gtf file from flybase.org (r6.32) using parameters: annot.ext = gtfPath,
60 isGTFAnnotationFile = T, isPairedEnd = T, strandSpecific = 1, nthreads = 4, GTF.featureType = 'exon',
61 allowMultiOverlap = F³. DESeq2 (v1.26.0) was used to identify differentially expressed genes using the
62 lfcShrink function to shrink log-fold changes and with each genotype and time-point as a separate
63 contrast⁴. Differentially expressed genes were defined as genes with an adjusted p-value less than 0.05
64 and an absolute log₂ fold change greater than 1. Normalized counts were generated using the counts
65 function in DESeq2. For c-means clustering, normalized counts were first converted into the fraction of
66 maximum normalized counts across all tissues and conditions and c-means clustering was performed
67 using the ppclust package (v1.1.0)⁵. MA Plots were made with ggplot2 and points were shaded using
68 kernel density estimates calculated using the MASS (v7.3-51.4) package⁶. Heatmaps were generated
69 using ggplot2 (v3.3.2) and patchwork (v1.1.0) in R⁷⁻⁹. Gene Ontology (GO) analysis was performed
70 using Bioconductor packages TopGO (v2.38.1) and GenomicFeatures (v1.38.2) using expressed genes
71 as a background set with parameters: algorithm = 'elim' and statistic = 'fisher'¹⁰. Similar GO terms were

72 collapsed based on semantic similarity using the rrvgo package in R and only the parent term was used
73 (v1.1.1)¹¹. Expressed genes were defined as genes with a normalized count value ≥ 10 .

74 **CUT&RUN Sequencing Analysis**

75 Technical replicates were merged by concatenating fastq files. Reads were trimmed using bbmap
76 (v38.75) with parameters ktrim=r ref=adapters rcomp=t tpe=t tbo=t hdist=1 mink=11. Trimmed reads
77 were aligned to the dm6 reference genome using Bowtie2 (v2.2.8) with parameters --local --very-
78 sensitive-local --no-unal --no-mixed --no-discordant --phred33 -I 10 -X 700¹². Reads with a quality score
79 less than 5 were removed with samtools (v1.9)¹³. PCR duplicates were marked with Picard (v2.21) and
80 then removed with samtools. Fragments between 20 and 120bp were isolated using a custom awk script
81 and used for downstream analyses as recommended in¹⁴. Bam files were converted to bed files with
82 bedtools (v2.29) with parameter -bedpe¹⁵. Bedgraphs were generated with bedtools and then converted
83 into bigwigs with ucsc tools (v320)¹⁶. Data was z-normalized using a custom R script. MACS (v2.1.2)
84 was used to call peaks on individual replicates and merged files using parameters -g 137547960--
85 nomodel --seed 123¹⁷. As a control for peak calling, wing IgG supernatant and pellet samples were used.
86 Wing IgG controls were *yw* CUT&RUN samples in which the primary antibody was omitted and only
87 the mouse anti-Rabbit IgG secondary was used. To identify differentially bound regions, a union peak
88 set was generated and RSubread (v2.0.1) was used to assign to features using parameters strandSpecific
89 = 0, allowMultiOverlap = T and then used as input for DESeq2 (v1.26.0)^{3,4}. To identify sites that were
90 differentially bound in each tissue irrespective of whether they were found in the supernatant or pellet
91 samples (see Sample Preparation for CUT&RUN), we entered the DESeq2 design formula as, “~tissue
92 + supPel”. For pairwise comparisons, union peaks were subsequently filtered to contain peaks that
93 overlapped a peak found in either sample by at least one base pair. MA plots were made as described for
94 RNAseq. Heatmaps and average signal plots were generated from z-normalized data using the
95 Bioconductor package Seqplots (v1.24.0) and plotted using ggplot2¹⁸. ChIPpeakAnno (v3.20.0) was used

96 to calculate distance of peaks to their nearest gene¹⁹. To identify clusters of EcR binding sites, the EcR
97 peaks were resized to 5000bp, assigned to clusters, and the furthest start and end coordinate of the original
98 peaks were used.

99 **FAIRE sequencing analysis**

100 Technical replicates were merged by concatenating fastq files. Reads were trimmed using bbmap
101 (v38.75) with parameters ktrim=r ref=adapters rcomp=t tpe=t tbo=t hdist=1 mink=11. Trimmed reads
102 were aligned to the dm6 reference genome using Bowtie2 (v2.2.8) with parameters --phred33 --seed 123
103 -x¹². Reads with a quality score less than 5 were removed with samtools (v1.9)¹³. PCR duplicates were
104 marked with Picard (v2.21) and then removed with samtools. Fragments smaller than 120bp were
105 removed from salivary gland datasets to correct for differences in signal-to-noise between wing and
106 salivary gland samples. The remaining processing and analysis steps were performed as described for
107 CUT&RUN.

108 **Motif Analysis**

109 To identify occurrences of the EcR motif in the genome, PWMs for the EcR and Usp motifs identified
110 by a bacterial 1-hybrid were obtained from Fly Factor Survey²⁰. For the palindromic, Usp/EcR motif, the
111 PWMs for EcR and Usp were concatenated together and the probabilities for the central, overlapping
112 base were averaged. FIMO (v4.12.0) was run on the dm6 reference genome using parameters --max-
113 stored-scores 10000000 --max-strand --no-qvalue --parse-genomic-coord --verbosity 4 --thresh 0.01²¹.
114 Motif density plots were generated by counting the number of motifs from peak summits (10bp bins) and
115 normalizing by the number of input peaks. Differential motif enrichment +/- 150bp from the summit of
116 EcR and FAIRE peaks was performed using the 'calcBinnedMotifs' function in monaLisa²² and the
117 JASPAR motif database²³.

118 **EcR knockdown in the wing and salivary gland**

119 To knockdown EcR in the wing and salivary gland in parallel, we made use of the previously published
120 line: *yw; vg-GAL4, UAS-FLP, Tub>>STOP>>GAL4, UAS-GFP / CyO*. Early activation of *vg-GAL4*
121 throughout the wing primordia results in flip-out of the stop-cassette and persistent expression of *Tub-*
122 *GAL4* throughout wing development. This construct is also active in the salivary gland during the first
123 larval instar stage, which may be a consequence of the *vg-GAL4* p-element vector which has been
124 previously reported to have a minimal promoter active in the salivary gland.

125 **Drosophila culture and genetics**

126 Flies were grown at 25C under standard culture conditions. Late wandering larvae were used as the –
127 6hAPF timepoint. White prepupae were used as the 0h time point for staging +6hAPF animals. For
128 staging –30hAPF, apple juice plates with embryos were first cleared of any larvae. Four hours later, any
129 animals that had hatched were transferred to vials. 72 hours later, tissues were harvested. The following
130 genotypes were used:

131 *yw; vg-GAL4, UAS-FLP, UAS-GFP, Tub>CD2>GAL4 / CyO*.

132 *w1118; P[UAS-EcR-RNAi]104 (BDSC#9327)*

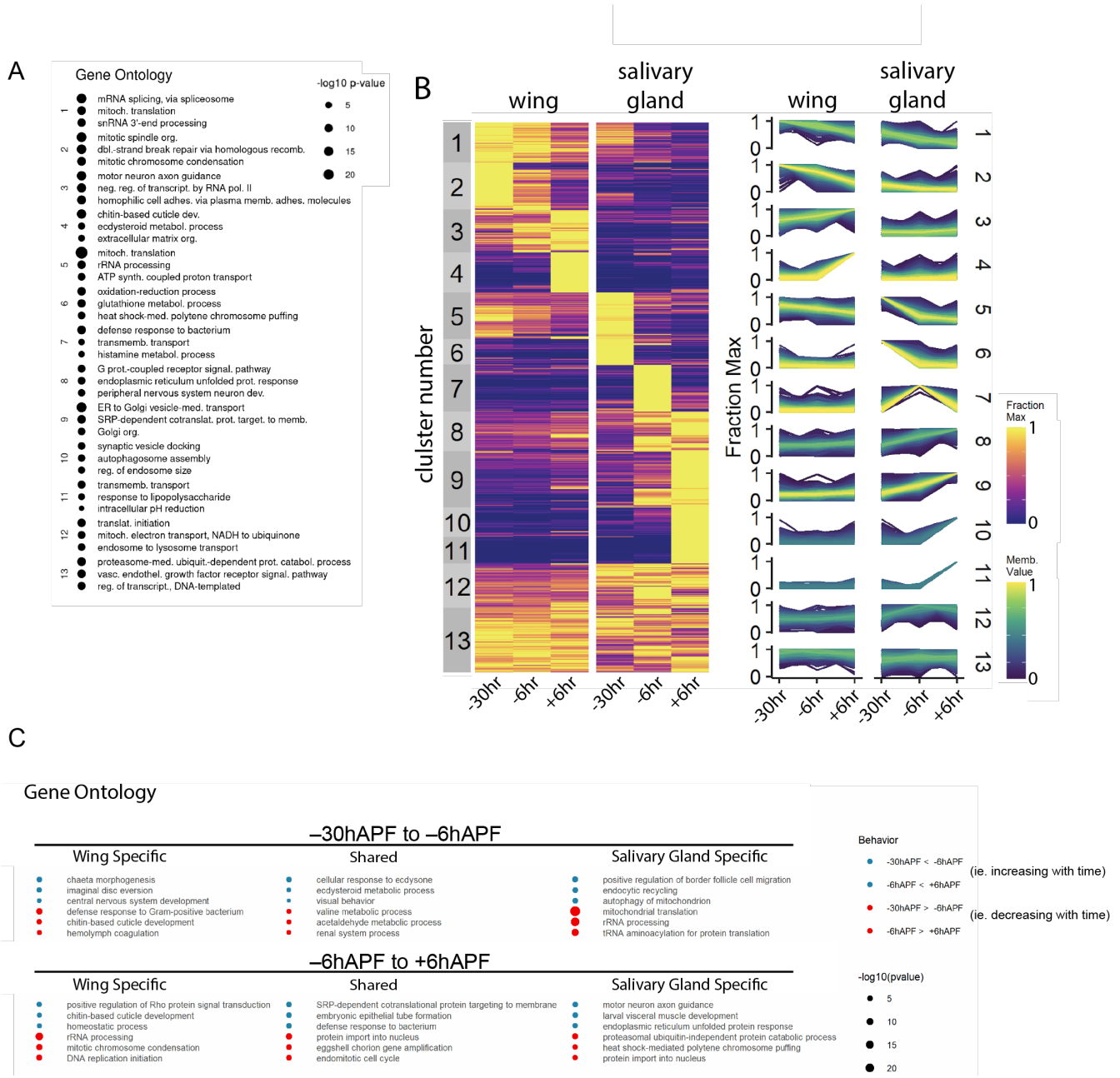
133 *yw; EcR^{GFSTF} (BDSC#59823)*

134 *w1118; Df(2R)BSC313 /CyO (BDSC#32253)*

135 *yw; + / + ; br^{disc}::tdTomato / TM6B*

136 *yw; +/+; E74_A-I::tdTomato/TM6B*

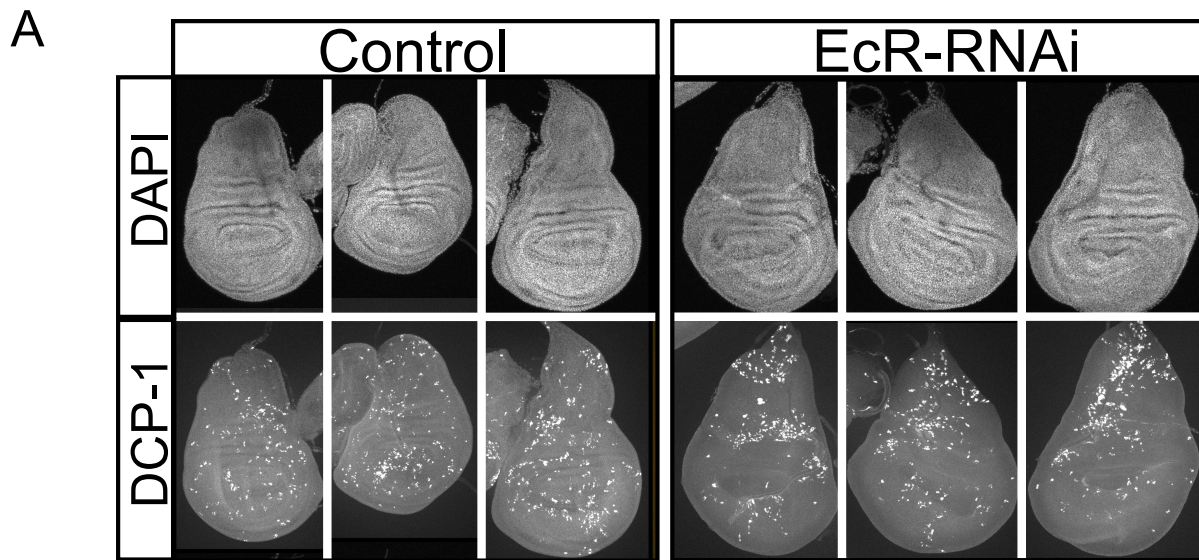
137



138

139 **Figure S1.** Gene ontology of temporally dynamic genes in wings and salivary glands. (A) Gene ontology
 140 terms for each cluster of genes depicted in the heatmap shown in Figure 1B. (B) Copy of the heatmap
 141 RNA-seq clusters shown in Figure 1B. (C) Gene ontology terms for temporally dynamic genes between
 142 adjacent time points in wild-type wings and salivary glands; these are the same genes depicted in the
 143 Venn diagram shown in Figure 1C.

144



B

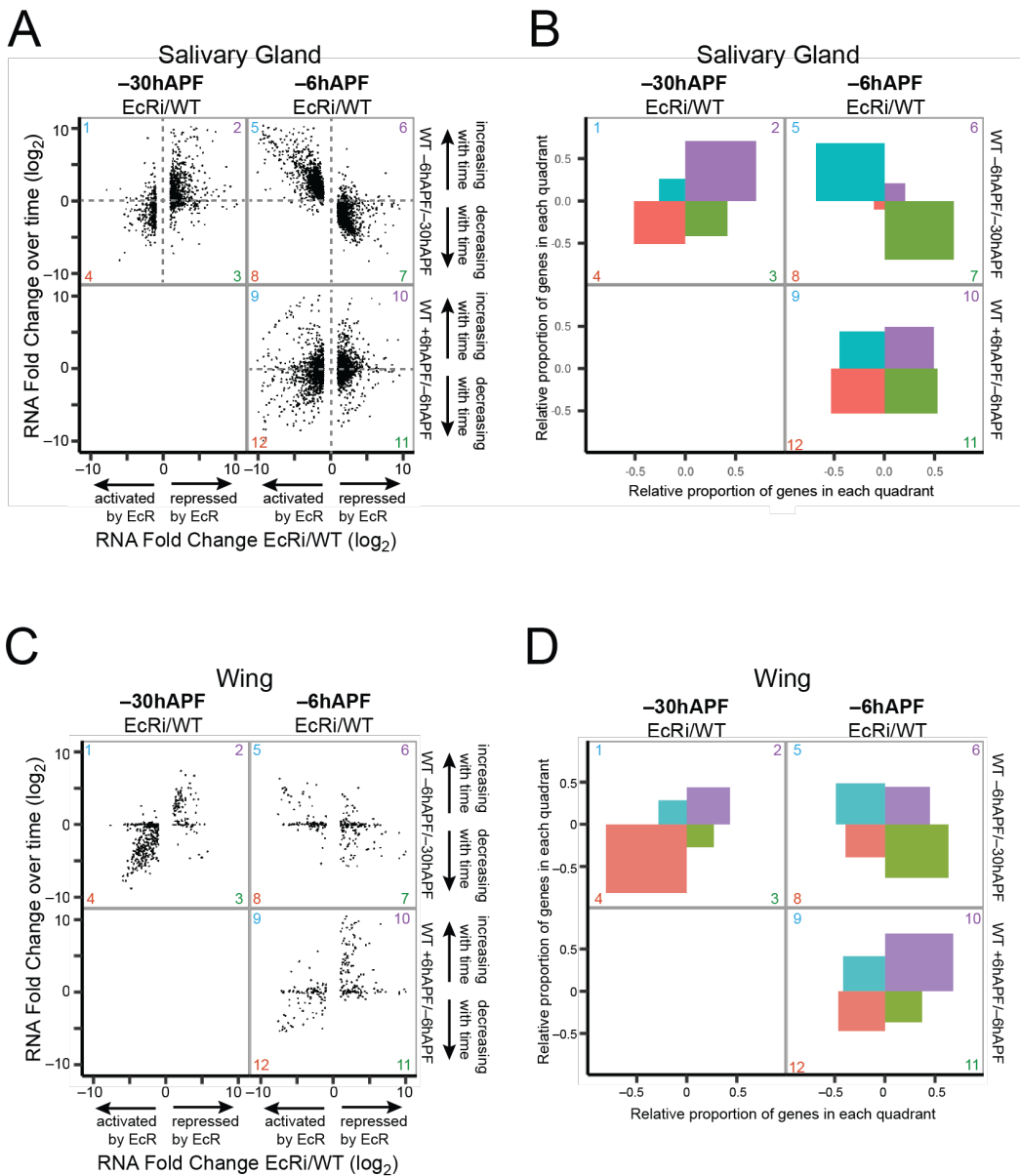
	Number salivary gland nuclei	
	control	EcR-RNAi
mean	122.6	123.0
standard deviation	11.9	10.6

C

	DNA content and size of salivary gland nuclei				
	DAPI mean	area	perimeter	feret diameter max	feret diameter min
control	105.52	618.42	94.02	34.63	23.97
EcR-RNAi	82.54	317.67	66.37	23.10	18.01
EcRi/WT	78%	51%	71%	67%	75%

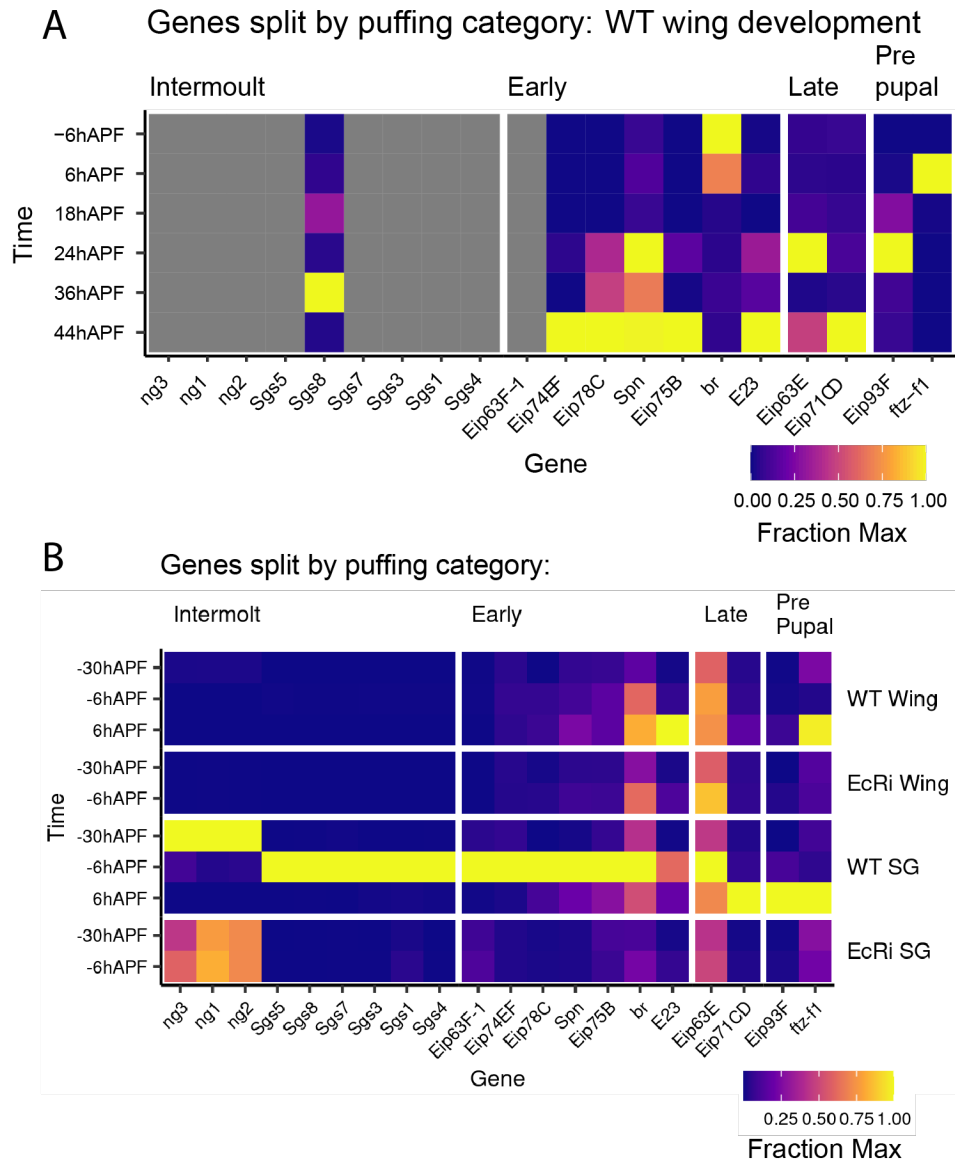
145

146 **Figure S2.** EcR loss of function does not increase cell death but disrupts proper polyteny. (A) Confocal
 147 images of DAPI and Dcp-1 staining from control (GAL4-only) and *EcR-RNAi* third instar wing imaginal
 148 discs. (B) Table of the number of nuclei from control (no GAL4 driver) and *EcR-RNAi* –6hAPF salivary
 149 glands (n = 12 control glands, n = 13 *EcR-RNAi* glands were scored). (C) Table of the DAPI signal
 150 (arbitrary units) and dimensions (pixels) for control (no GAL4 driver) and *EcR-RNAi* –6hAPF salivary
 151 glands (n = 47 nuclei from 9 control glands were scored, and n = 58 nuclei from 11 *EcR-RNAi* glands
 152 were scored).



153

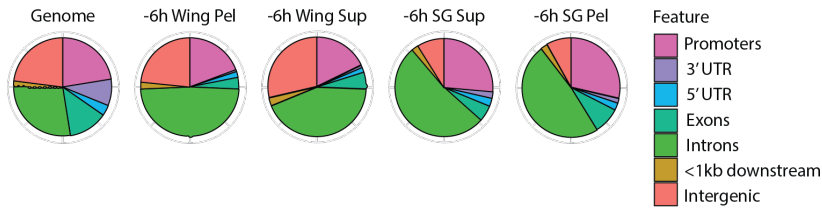
154 **Figure S3.** EcR is required for both gene activation and gene repression at -30hAPF and at -6hAPF in
 155 wings and salivary glands. (A) and (B) Copies of the scatterplots and gene proportion plots from Figure
 156 2C, D. (C) Scatterplots of RNA-seq values for differentially expressed genes in *EcR-RNAi* wings. The
 157 ratio between *EcR-RNAi* and wild-type is shown on the x-axis for -30hAPF and -6hAPF. The ratio
 158 between adjacent wild-type stages is shown on the y-axis. (D) Plots indicating the proportion of genes
 159 located in each quadrant for the three scatterplots shown in Panel C.



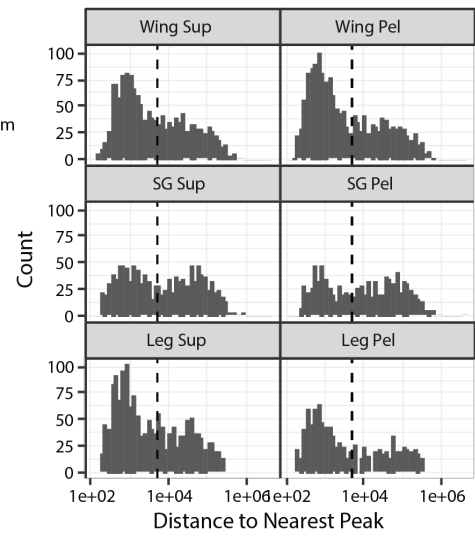
160

161 **Figure S4.** Expression of genes residing in puffing loci from developing wings. (A) Heatmap of RNA-
 162 seq values (fraction of max) from a wild-type wing developmental time course for select genes that
 163 exhibit ecdysone-dependent puffs in the salivary gland. (B) Heatmap of RNA-seq values (fraction of
 164 max) from wild-type and *EcR-RNAi* tissues for select genes that exhibit ecdysone-dependent puffs in
 165 salivary glands.

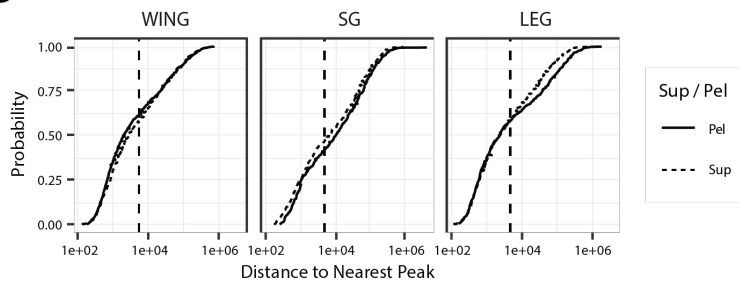
166

A**B**

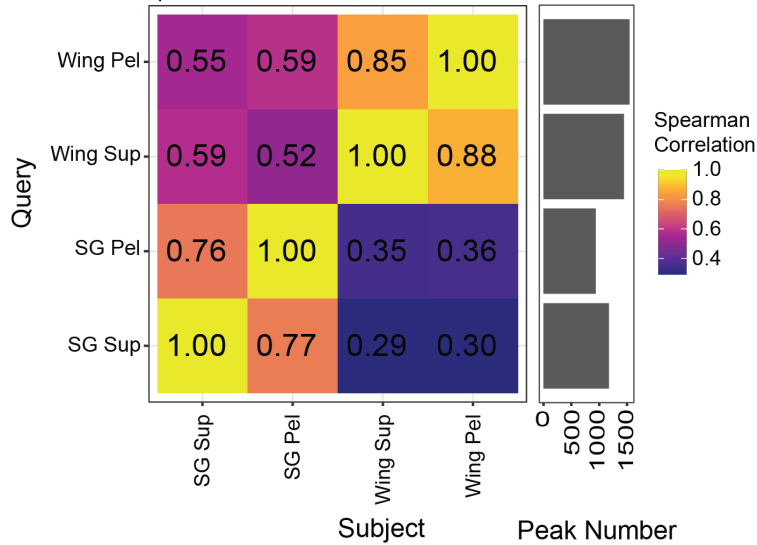
Histogram of distance to nearest peak within each peakset

**C**

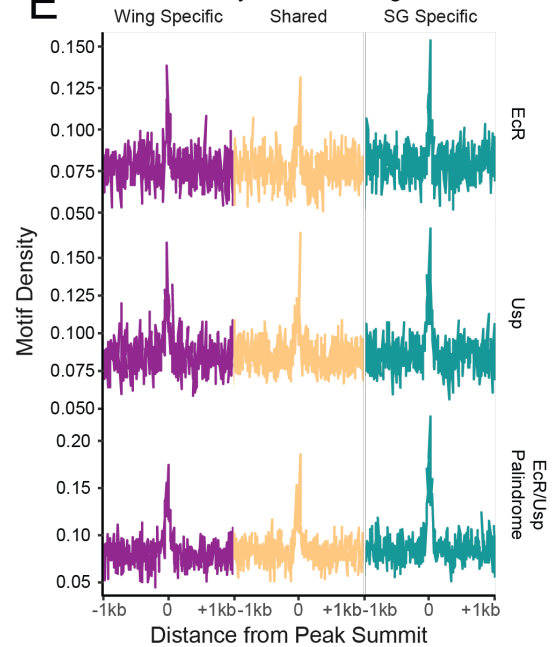
Cumulative dist to nearest peak within each peakset

**D**

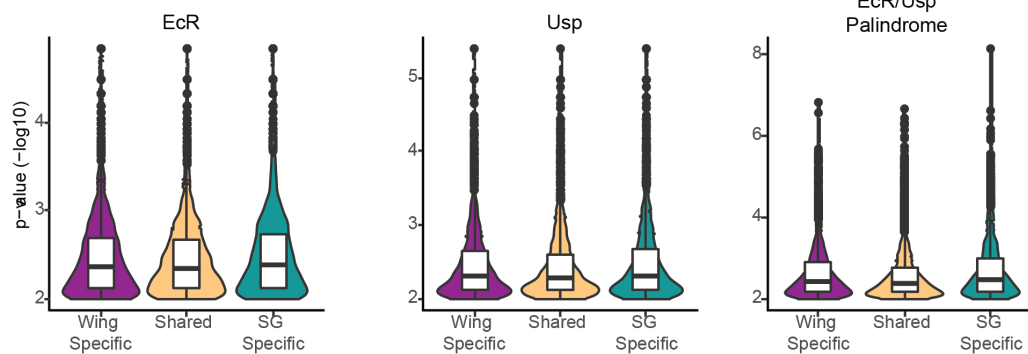
Correlation of signal within peaks
Spearman correlation; RPGC normalized

**E**

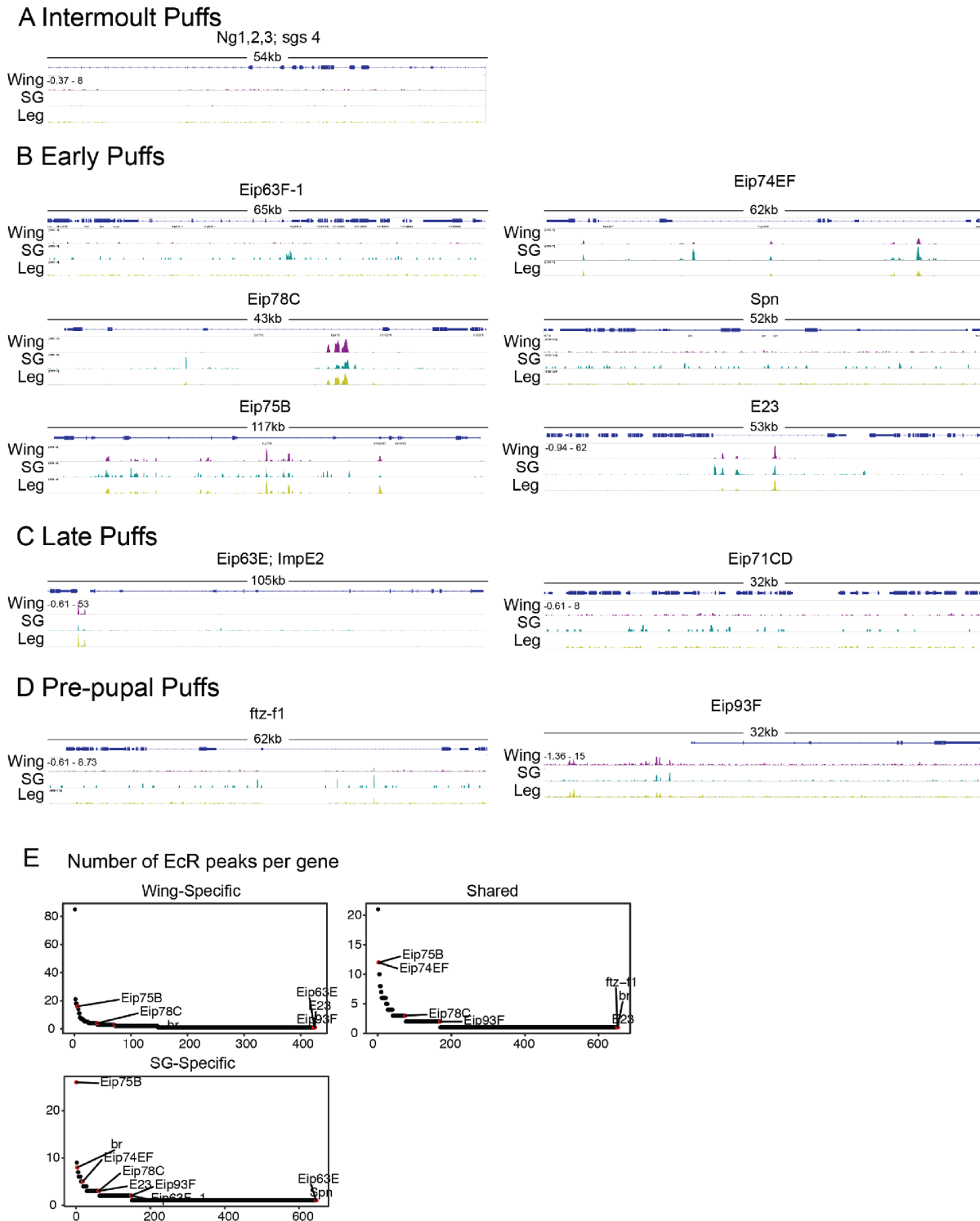
Motif Density in EcR Binding Sites

**F**

Motif Quality in EcR Peaks



168 **Figure S5.** Additional properties of EcR binding sites. (A) Pie charts of the genome-wide distribution of
169 EcR binding sites. (B) Histograms and (C) cumulative distribution plots of the distance of each EcR peak
170 to its nearest neighbor. Peaks falling within 5kb (dotted lines) of each other define an EcR cluster. (D)
171 Heatmap of the Spearman correlation coefficient for EcR CUT&RUN signal within EcR peaks between
172 tissues and separated by whether the supernatant (sup) or pellet (pel) DNA was sequenced following the
173 CUT&RUN protocol (see Methods). (E) Line plots of motif density surrounding the summit (+/- 1kb) of
174 EcR CUT&RUN peaks. Individual EcR and Usp motifs from Fly Factor Survey were used, as well as an
175 EcR/Usp palindrome that was generated by combining EcR and Usp motifs. (F) Violin plots of p values
176 for sequences matching EcR, Usp individual motifs, or the EcR/Usp palindrome.
177



178

179

180

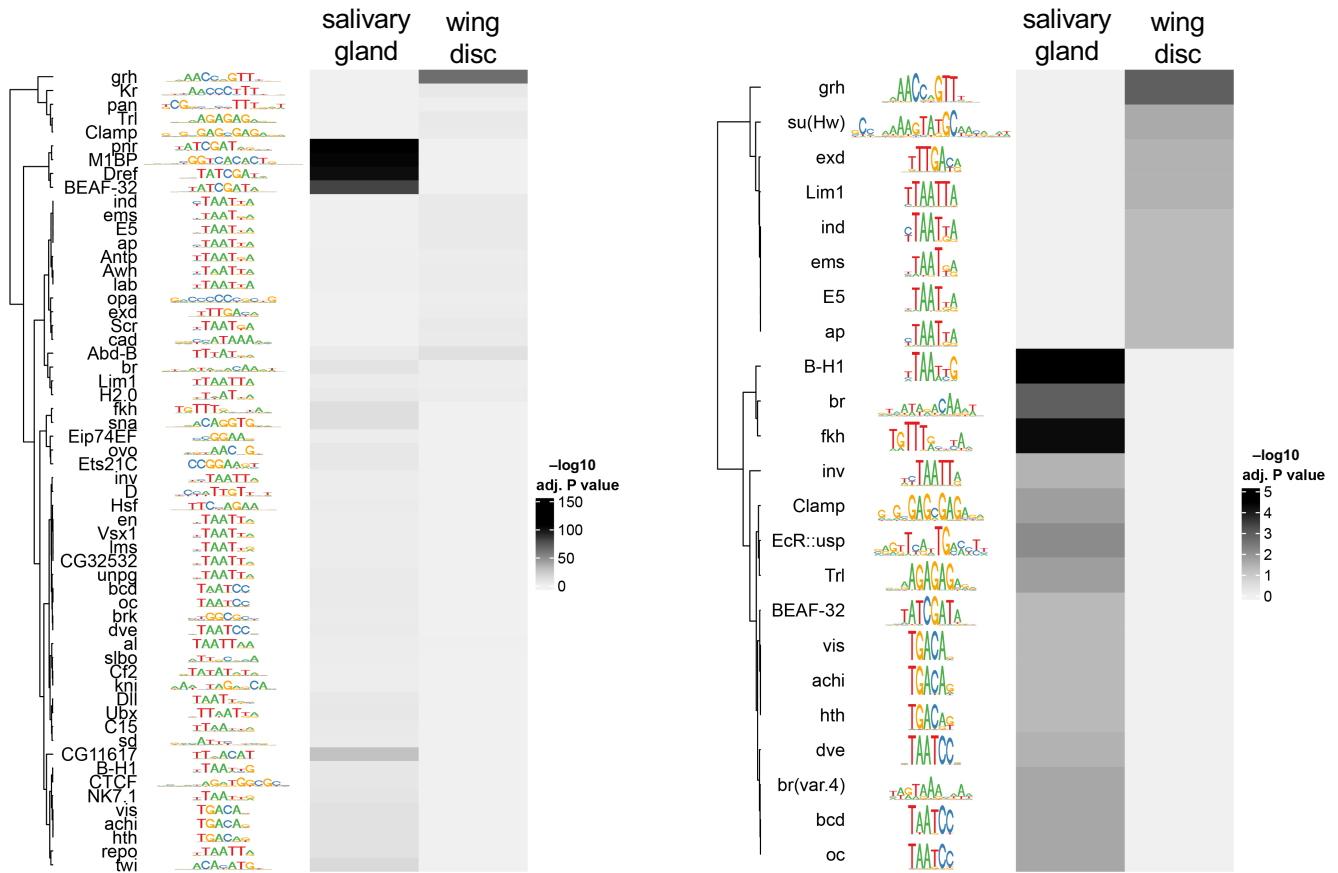
181

182

Figure S6. EcR binds extensively near ecdysone primary response genes using a mixture of tissue-specific and shared binding sites. (A-D) Browser shots of EcR CUT&RUN signal in wings and salivary glands at puffing loci. (E) Ranked plots of EcR peak number at wing-specific, shared, and salivary gland-specific EcR CUT&RUN peaks. Puffing genes are indicated and highlighted in red.

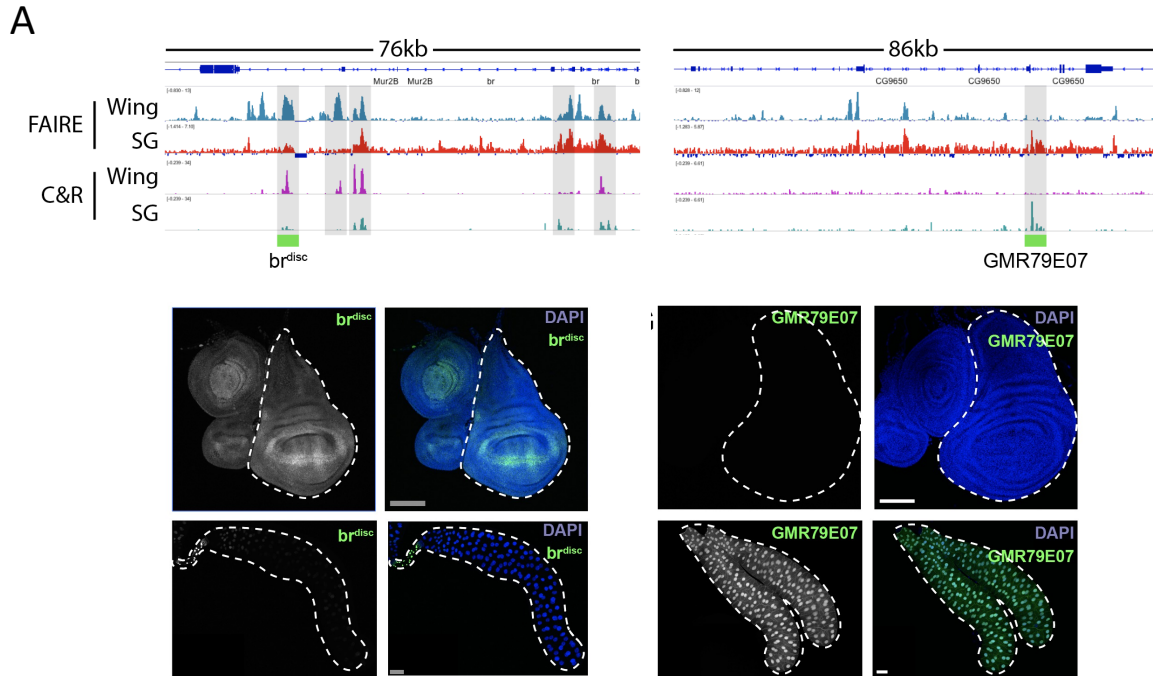
Relative motif enrichment in FAIRE peaks

Relative motif enrichment in EcR CUT&RUN peaks



183

184 **Figure S7.** Relative motif enrichment in FAIRE peaks and EcR binding sites. Heatmaps of relative motif
 185 enrichment ($-\log_{10}$ adjusted p value) in tissue-specific FAIRE peaks (left) and tissue-specific EcR
 186 CUT&RUN peaks (right) from salivary glands and wing imaginal discs. The matching transcription
 187 factor and its motif are shown alongside. Similar motifs are hierarchically clustered by Pearson
 188 correlation.



B
E74 Enhancers

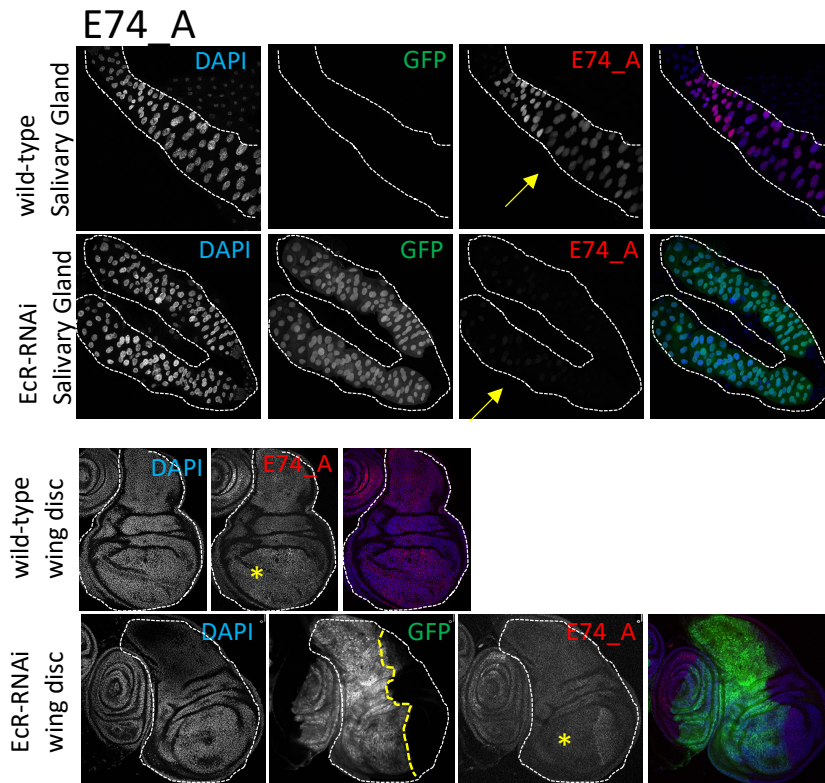


Figure S8

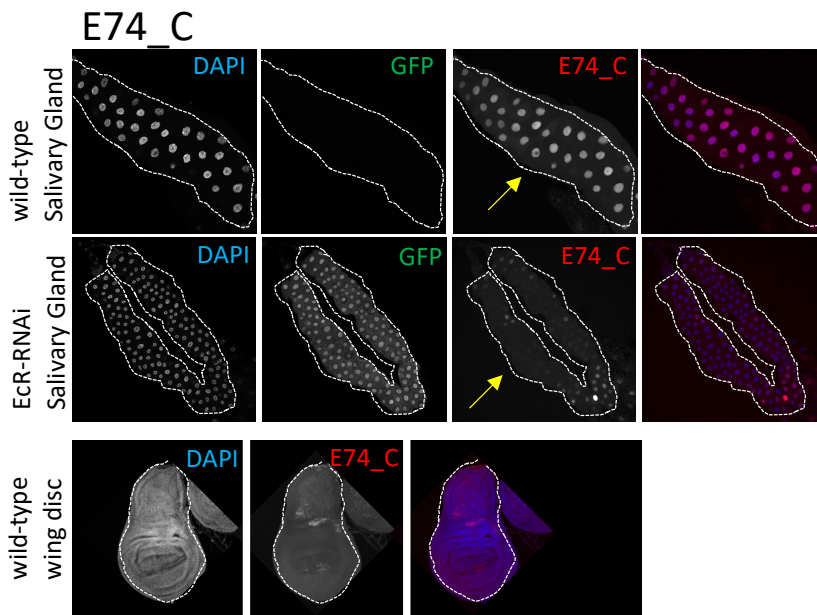
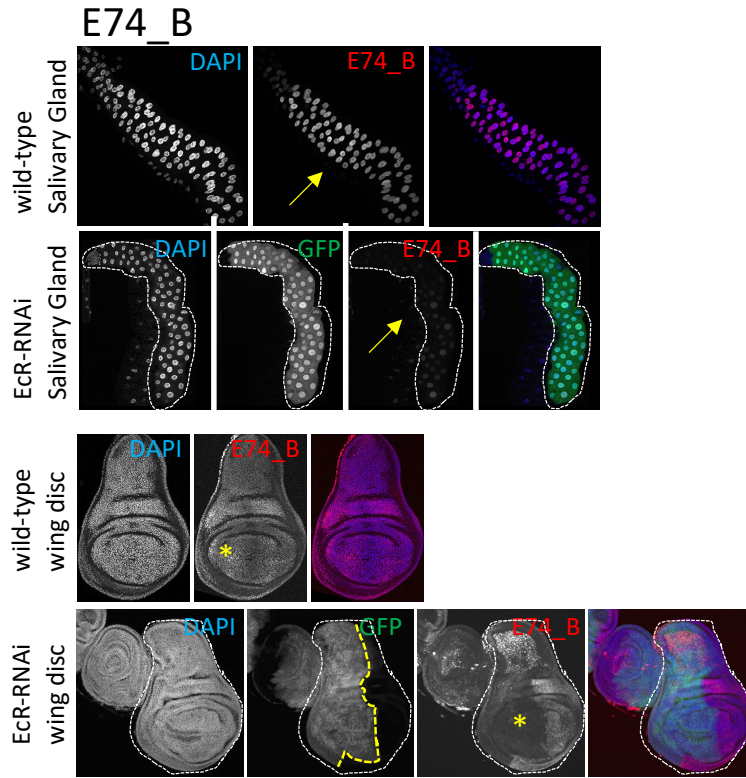


Figure S8

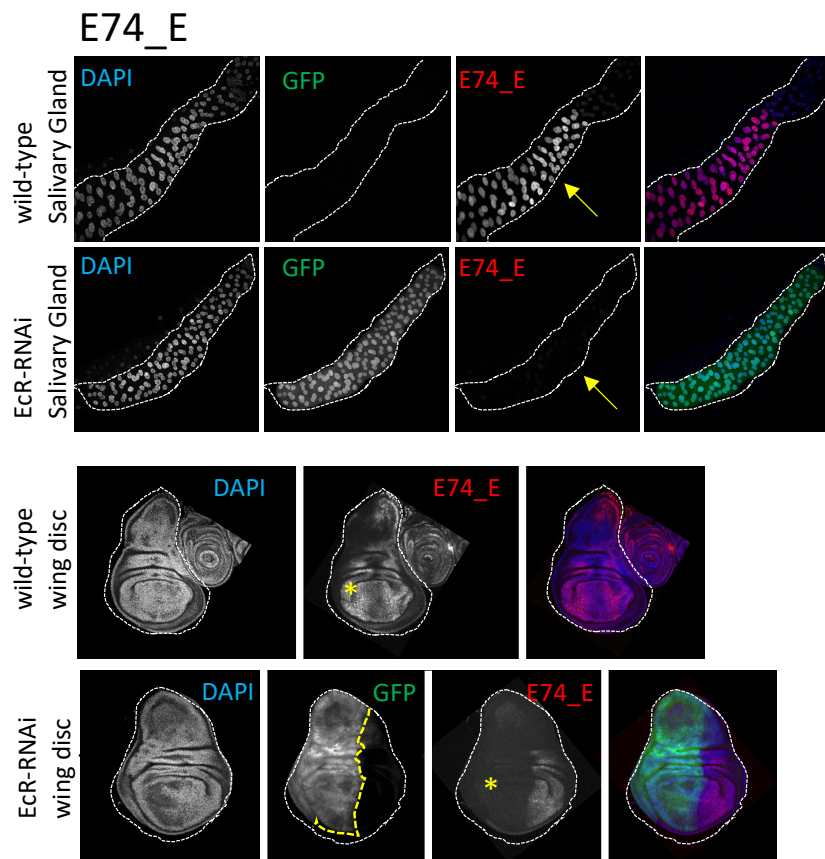
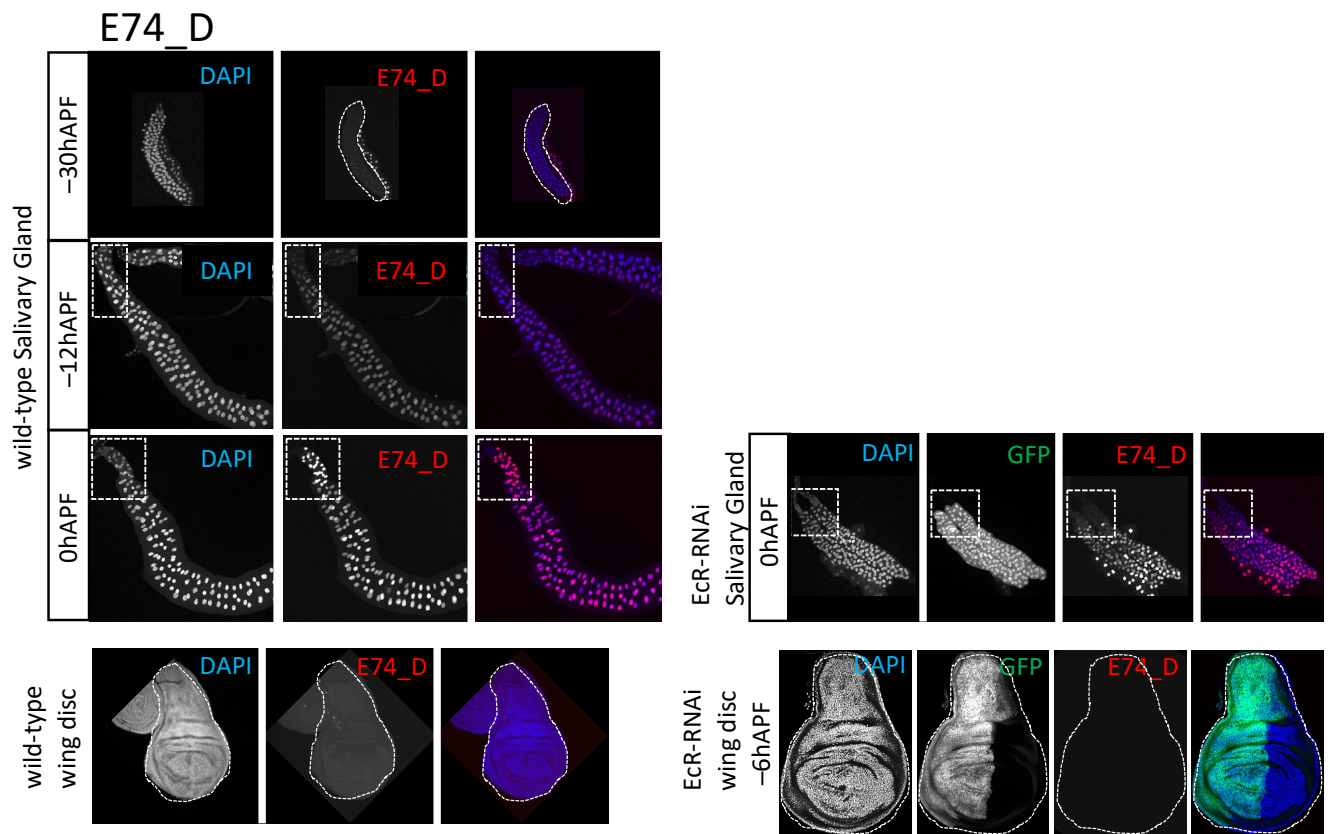


Figure S8

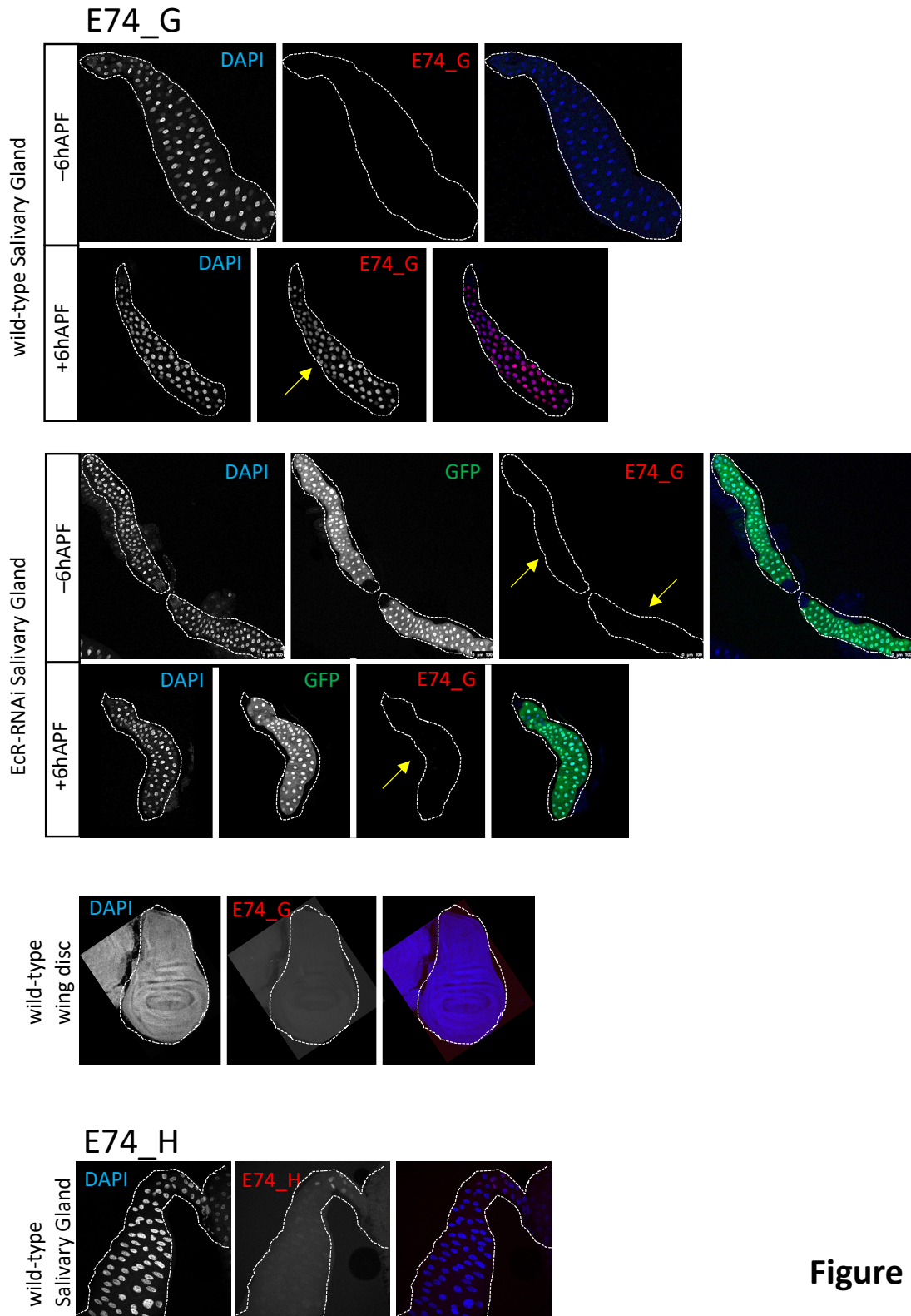
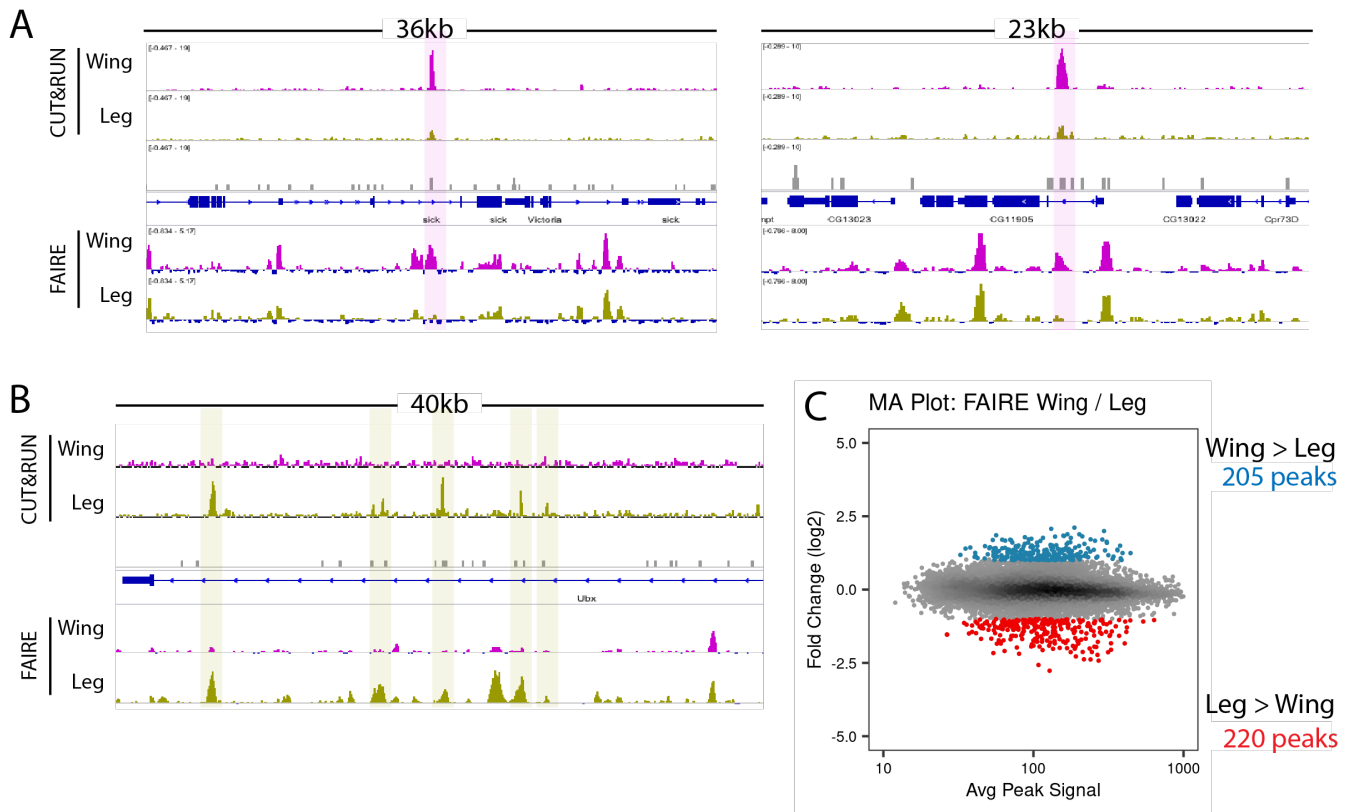


Figure S8

193 **Figure S8.** EcR binding sites correspond to active enhancers. (A) Browser shots of FAIRE and EcR
194 CUT&RUN signal from –6hAPF wings and salivary glands for genomic loci surrounding the *br^{disc}* and
195 *GMR79E07* enhancers. Confocal images depict enhancer activity (green) and DAPI (blue) in wild-type
196 wings and salivary glands from the same developmental stage. (B) Confocal images of *E74* enhancer
197 activity in wild-type wings and salivary glands. Enhancer activity is visualized by tdTomato expression
198 (red), DNA by DAPI stain (blue). For *EcR-RNAi* tissues, the expression of the GAL4 driving *UAS-EcR-*
199 *RNAi* is captured by *UAS-GFP* (green). Yellow lines in wing discs indicate the boundary between *Ci-*
200 *GAL4* expressing and wild-type cells. Developmental stage is –6hAPF for all images, except when
201 indicated on the left. Yellow asterisks indicate loss of enhancer activity relative to wild-type wings.
202 Yellow arrows indicate loss of enhancer activity relative to wild-type salivary glands. For *E74_D*, the
203 white dashed box highlights the transition cells, which exhibit the strongest dependence on EcR for
204 enhancer activity. In wild-type glands, *E74_D* enhancer activity increases in transition cells during the
205 larval-to-prepupal transition; however, in *EcR-RNAi* cells, the enhancer fails to increase in activity in
206 these cells.
207



208

209 **Figure S9.** Differential EcR binding between wings and legs overlaps sites of differential accessibility.

210 (A) Browser shots of EcR CUT&RUN and FAIRE signal from -6hAPF wings and legs at loci that exhibit

211 wing-specific EcR peaks. (B) Browser shots of EcR CUT&RUN and FAIRE signal from wings and legs

212 at loci that exhibit leg-specific EcR peaks. (C) MA plot of FAIRE signal in -6hAPF wings and legs.

213 Differential peaks (absolute log₂ fold change > 1, adj p value < 0.05) are colored in blue and red.

214

215 References

- 216 1. Ahmad, K., *CUT&RUN with Drosophila tissues*, in
217 <https://doi.org/10.17504/protocols.io.umfeu3n>. 2018.
- 218 2. Dobin, A., et al., *STAR: ultrafast universal RNA-seq aligner*. Bioinformatics (Oxford, England),
219 2013. **29**(1): p. 15-21.
- 220 3. Liao, Y., G.K. Smyth, and W. Shi, *featureCounts: an efficient general purpose program for*
221 *assigning sequence reads to genomic features*. Bioinformatics (Oxford, England), 2014. **30**(7):
222 p. 923-30.
- 223 4. Love, M.I., W. Huber, and S. Anders, *Moderated estimation of fold change and dispersion for*
224 *RNA-seq data with DESeq2*. Genome biology, 2014. **15**(12): p. 550-550.
- 225 5. Cebeci, Z., *Comparison of internal validity indices for fuzzy clustering*. Journal of Agricultural
226 Informatics, 2019. **10**(2): p. 1-14.
- 227 6. Venables, W.N. and B.D. Ripley, *Modern Applied Statistics with S*. Fourth ed. 2002: Springer.
- 228 7. Pedersen, T.L., *patchwork: The Composer of Plots*, in *cran.r-project*. 2020.
- 229 8. Wickham, H., *ggplot2*. 2009, New York, NY: Springer New York.
- 230 9. Wickham, H., *A Layered Grammar of Graphics*. Journal of Computational and Graphical
231 Statistics, 2010. **19**(1): p. 3-28.
- 232 10. Alexa, A. and J. Rahnenfuhrer, *Enrichment Analysis for Gene Ontology*, in
233 *10.18129/B9.bioc.topGO*. 2018.
- 234 11. Sayols, S., *Reduce + Visualize GO*, in *10.18129/B9.bioc.rvgo*. 2020.
- 235 12. Langmead, B. and S.L. Salzberg, *Fast gapped-read alignment with Bowtie 2*. Nature methods,
236 2012. **9**(4): p. 357-9.
- 237 13. Li, H., et al., *The Sequence Alignment/Map format and SAMtools*. Bioinformatics (Oxford,
238 England), 2009. **25**(16): p. 2078-9.
- 239 14. Skene, P.J. and S. Henikoff, *An efficient targeted nuclease strategy for high-resolution mapping*
240 *of DNA binding sites*. eLife, 2017. **6**.
- 241 15. Quinlan, A.R. and I.M. Hall, *BEDTools: a flexible suite of utilities for comparing genomic*
242 *features*. Bioinformatics (Oxford, England), 2010. **26**(6): p. 841-2.
- 243 16. Kent, W.J., et al., *BigWig and BigBed: enabling browsing of large distributed datasets*.
244 Bioinformatics (Oxford, England), 2010. **26**(17): p. 2204-7.
- 245 17. Zhang, Y., et al., *Model-based analysis of ChIP-Seq (MACS)*. Genome biology, 2008. **9**(9): p.
246 R137-R137.
- 247 18. Stempor, P. and J. Ahringer, *SeqPlots - Interactive software for exploratory data analyses,*
248 *pattern discovery and visualization in genomics*. Wellcome open research, 2016. **1**: p. 14-14.
- 249 19. Zhu, L.J., et al., *ChIPpeakAnno: a Bioconductor package to annotate ChIP-seq and ChIP-chip*
250 *data*. BMC bioinformatics, 2010. **11**: p. 237-237.
- 251 20. Zhu, L.J., et al., *FlyFactorSurvey: a database of Drosophila transcription factor binding*
252 *specificities determined using the bacterial one-hybrid system*. Nucleic acids research, 2011.
253 **39**(Database issue): p. D111-7.
- 254 21. Grant, C.E., T.L. Bailey, and W.S. Noble, *FIMO: scanning for occurrences of a given motif*.
255 Bioinformatics (Oxford, England), 2011. **27**(7): p. 1017-8.
- 256 22. Machlab, D., et al., *monaLisa: an R/Bioconductor package for identifying regulatory motifs*.
257 Bioinformatics, 2022.
- 258 23. Fornes, O., et al., *JASPAR 2020: update of the open-access database of transcription factor*
259 *binding profiles*. Nucleic Acids Res, 2020. **48**(D1): p. D87-D92.
- 260